HHS Public Access

Author manuscript

Proc SPIE Int Soc Opt Eng. Author manuscript; available in PMC 2016 April 04.

Published in final edited form as:

Proc SPIE Int Soc Opt Eng. 2016 March 7; 9701: 970106–. doi:10.1117/12.2211110.

Deformable medical image registration of pleural cavity for photodynamic therapy by using finite-element based method

Rozhin Penjweini[a], **Michele M. Kim**[a,b], **Andrea Dimofte**[a], **Jarod C Finlay**[a], and **Timothy C. Zhu**[a,*]

[a]Department of Radiation Oncology, School of Medicine, University of Pennsylvania, Philadelphia, PA 19104, USA

[b]Department of Physics and Astronomy, University of Pennsylvania, Philadelphia, PA 19104, USA

Abstract

When the pleural cavity is opened during the surgery portion of pleural photodynamic therapy (PDT) of malignant mesothelioma, the pleural volume will deform. This impacts the delivered dose when using highly conformal treatment techniques. To track the anatomical changes and contour the lung and chest cavity, an infrared camera–based navigation system (NDI) is used during PDT. In the same patient, a series of computed tomography (CT) scans of the lungs are also acquired before the surgery. The reconstructed three-dimensional contours from both NDI and CTs are imported into COMSOL Multiphysics software, where a finite element-based (FEM) deformable image registration is obtained. The CT contour is registered to the corresponding NDI contour by overlapping the center of masses and aligning their orientations. The NDI contour is considered as the reference contour, and the CT contour is used as the target one, which will be deformed. Deformed Geometry model is applied in COMSOL to obtain a deformed target contour. The distortion of the volume at X, Y and Z is mapped to illustrate the transformation of the target contour. The initial assessment shows that FEM-based image deformable registration can fuse images acquired by different modalities. It provides insights into the deformation of anatomical structures along X, Y and Z-axes. The deformed contour has good matches to the reference contour after the dynamic matching process. The resulting three-dimensional deformation map can be used to obtain the locations of other critical anatomic structures, e.g., heart, during surgery.

Keywords

PDT; image deformable registration; CT; NDI; finite element-based method; mesothelioma; lung and chest cavity

1. INTRODUCTION

Deformable image registration is used in radiation therapy, image-guided surgery, functional magnetic resonance images (MRI) analysis, and tumor detection, as well as many nonmedical applications, such as computer vision, pattern recognition, and remotely sensed

*tzhu@mail.med.upenn.edu; phone 215-662-4043.

data processing.[1–3] The process of deformable image registration consists of establishing spatial correspondences between different image acquisitions.[4] The term “deformable” denotes the fact that the observed signals are associated through a non-linear dense transformation, or a spatially varying deformation model. The most important applications of deformable image registration are: i) multi-modality fusion, where information acquired by different imaging devices or protocols is fused to facilitate diagnosis and treatment planning; ii) longitudinal studies, where temporal structural or anatomical changes are investigated; and iii) population modeling and statistical atlases, which are used to study normal anatomical variability.

Type II photodynamic therapy (PDT) is a safe and noninvasive treatment modality that effectively kills cancer cells.[5, 6] PDT is based on the use of photochemical reactions mediated through an interaction between a photosensitizing drug (photosensitizer), photoexcitation with a specific wavelength of light, and massive production of reactive singlet oxygen, which is thought to be the major mechanism behind tumor cell killing.[6, 7] PDT is currently coupled with surgical resection of the malignant pleural mesothelioma tumor as a local treatment suitable to treat the microscopic disease and to increase survival rates.[8] Although accurate light dosimetry is imperative to treatment efficacy, the deformation of the pleural volume during the surgery when the pleural cavity is opened impacts the delivered dose. In this study, to track the anatomical changes and contour the lung and chest cavity, an infrared camera–based navigation system (NDI) is used during PDT.[8, 9] In the same patient, a series of computed tomography (CT) scans of the lungs are also acquired before the surgery. Then, finite element-based (FEM) deformable image registration[4, 10] is used to quantify the anatomical variation between the contours for the pleural cavities obtained in the operating room and those determined from pre-surgery CTs.

2. METHODS

2.1 Obtaining the volume of lung prior to the surgery and PDT

A series of CTs of the lungs was acquired before the surgery at the Hospital of the University of Pennsylvania. The three dimensional (3D) volume of the lung obtained from the CTs were processed and contoured using Aria, Matlab and MeshLab software (see Fig. 1).

2.2 Obtaining the volume of lung and plural cavity during PDT

Light delivery information was obtained during treatment so that it can be used to display the cumulative light fluence on every point of the cavity surface that is being treated. The treatment delivery wand is comprised of a modified endotrachial tube filled with scattering media and an optical fiber inside the tube to deliver the laser light. The position of the treatment is tracked using an attachment that has nine reflective passive markers that are seen by the IR camera (see Figs. 2(a) and (b)). The collected position points were processed and plotted as a three dimensional volume of the pleural cavity using Matlab and MeshLab software as shown in Fig. 2(c).[8, 9, 11]

2.3 Matching of the orientation of the NDI and CT volumes

During surgery, the laser delivery wand with the NDI passive markers were used to determine the “standard” orientation along the patient. The wand was briefly held above and parallel to the patient, with the passive markers towards the head of the patient. This coordinate was used to orient the NDI volume obtained during treatment so that the top of the treatment volume is upwards on the z-axis. A 3×3 rotational matrix (M_{std}) defines the orientation of the treatment wand in the “standard” orientation, and all measured volume coordinates are transformed using M_{std}.[9]

2.4 Deformable image registration using COMSOL Multiphysics

The CT and NDI volumes were imported into COMSOL Multiphysics 5.0, where the FEM-based deformable image registration is obtained. The volumes of the NDI and CT domains were calculated to be 2360 and 2060 cm^3, respectively. The contours were registered by overlapping their center of masses and orientations (see Fig. 3(a)). Lung stress-strain material properties needed for this model are density, Poisson's value and Young’s modulus. The stress-strain material properties of lung have been shown in Table 1. A more detailed description of the lung tissue properties can be found elsewhere.[12–14]

FEM involves dividing the domain of the problem into a collection of subdomains, with each subdomain represented by a set of element equations to the original problem, followed by systematically recombining all sets of the element equations into a global system of equations for the final calculation. The global system of equations has known solution techniques, and can be calculated from the initial values of the original problem to obtain a numerical answer. Fig. 3(b) and Table 2 show the FEM analyses mesh properties generated for the CT and NDI contours.

In our model, the subdomain mesh displacement was set as free displacement. The NDI acquired contour is considered as the reference, and the CT contour is used as the target, which will be deformed by introducing a Deformed Geometry interface. The shear modulus, G, can be computed from Young’s modulus, E, and Poisson’s ratio, v, as

$$G=\frac{E}{2(1+v)} \quad (1)$$

The bulk modulus, K, which measures the change in volume for a given uniform pressure can be expressed as

$$K=\frac{E}{3(1-2v)} \quad (2)$$

For small deformations, most elastic materials exhibit linear elasticity and can be described by a linear relation between the stress, σ, and strain, ε

$$\sigma=E\varepsilon \quad (3)$$

In continuum mechanics, a Hypoelastic material, which is an elastic material that has a constitutive model independent of finite strain measures except in the linearized case is described by a relation of the form

$$\overset{\bullet}{\sigma} = D : \overset{\bullet}{F} \quad (4)$$

where, D is the material property tensor, F is the deformed gradient and superposed dots indicate time derivatives, $\partial/\partial t$.

In many solid mechanics problems, material deformation is characterized by a small (or linearized) strain tensor

$$\varepsilon_{ij} = \frac{1}{2}(u_{i,j} + u_{j,i}) \quad (5)$$

where u_i are the components of the displacements of continuum points, the subscripts refer to Cartesian coordinates (i=1, 2, 3) and the subscripts preceded by a comma denote partial derivatives (e.g., $u_{i,j} = \partial u_i/\partial x_j$).

For a sufficiently small loading step (or increment), one may use the deformation rate tensor (or velocity strain)

$$d_{ij} = \overset{\bullet}{\varepsilon}_{ij} = \frac{1}{2}(v_{i,j} + v_{j,i}) \quad (6)$$

or increment representing the linearized strain increment from the initial (stressed and deformed) state in the step

$$\Delta\varepsilon_{ij} = \overset{\bullet}{\varepsilon}_{ij}\, \Delta t = d_{ij}\Delta t \quad (7)$$

where, the dot represents the time derivative, Δ denotes a small increment over the time step, t, and $v_i = \overset{\bullet}{u}_i$ is the material point velocity or displacement rate.

The objective stress rate, $\widehat{\sigma_{ij}}$ and the corresponding increment $\Delta\sigma_{ij} = \widehat{\sigma_{ij}}\,\Delta t$ can also be introduced. $\widehat{\sigma_{ij}}$ is related to the element deformation and must be invariant with respect to coordinate transformations (particularly rotations) and must characterize the state of the same material element as it deforms.

3. RESULTS AND DISCUSSION

Image deformable registration is the process of determining the optimal spatial transformation that maps one image to another. In this study, the two 3D images obtained from the NDI system and CT that are respectively registered as the fixed and the moving images are the input to the registration algorithm. The output is the optimal transformation that maps the CT image to the NDI. In order to have accurate representation of our complex geometries, inclusion of dissimilar material properties, and easy representation of the total solution and capture of local effects we use FEM-based deformable registration.[10] Using a Deformed Geometry model in the Physics package of COMSOL, a linear stretching is

applied to the CT volume to distort the volume. The distortions in the X, Y and Z directions have been shown in Fig.4; different colors represent the different magnitudes of distortion.

Fig. 5(a) compares the CT contour with the NDI volume before the deformation and Fig. 5(b) shows the deformed CT contour as compared to the NDI volume; the images have been shown in four different orientations. A comparison of Figs. 5 (a) and 5 (b) shows that the lung volume delineated from the patient CT image can be artificially deformed using the FEM-based Deformed Geometry model. The volume of the deformed CT domain was calculated to be 2295 cm^3. Ideally, the transformed moving image should be identical to the fixed one after the registration. However, due to the big deformation of the lung during the surgery, there is a big difference between the CTs and the NDI volumes and the image deformable registration did not completely match the two contours. The deformed CT volume and the stress vectors in X, Y and Z have been shown in Fig. 5(c).

4. CONCLUSION AND FUTURE STUDIES

In this study, anatomical variation between the contours for the pleural cavities obtained in the operating room and those determined from pre-surgery CT scans could be quantified by using the FEM-based Deformed Geometry model in COMSOL. This preliminary study shows promising application of the FEM-based image deformable registration when images of the same object are taken at different times, from different imaging devices, or from different perspectives. We also showed that FEM is a good choice for analyzing problems over complicated domains, when the domain changes (as during a solid state reaction with a moving boundary), the desired precision varies over the entire domain, or the solution lacks smoothness. However, due to the big deformation of the lung during the surgery (NDI volume 2360 cm^3 compared to CT volume 2060 cm^3) our model did not completely match the two contours; the deformed CT volume was calculated to be 2295 cm^3. Future studies will be focused on using different physics for improving the accuracy of the technique.

Acknowledgments

The authors would like to thank all of the PDT group members at the Hospital of the University of Pennsylvania, Arjun G. Yodh, Carmen Rodriguez, Arash Darafsheh, Theresa M. Busch, Keith Cengel, Charles B Simone, Jess Appleton, Sally McNulty, Joann Miller, Min Yuan and Sunil Singhal. This work is supported by NIH grants R01 CA154562 and P01 CA87971.

REFERENCES

1. Sotiras A, Davatzikos C, Paragios N. Deformable medical image registration: a survey. IEEE transactions on medical imaging. 2013; 32(7):1153–1190. [PubMed: 23739795]
2. Paquin D, Levy D, Xing L. Multiscale deformable registration of noisy medical images. Mathematical biosciences and engineering: MBE. 2008; 5(1):125–144. [PubMed: 18193935]
3. Li J, Zhu TC. Deformable medical image registration using finite-element method. Proc. COMSOL. 2006
4. Liang J, Yan D. Reducing uncertainties in volumetric image based deformable organ registration. Medical physics. 2003; 30(8):2116–2122. [PubMed: 12945976]
5. Penjweini R, Loew H-G, Eisenbauer M, Kratky KW. Modifying excitation light dose of novel photosensitizer PVP-Hypericin for photodynamic diagnosis and therapy. Journal of photochemistry and photobiology B, Biology. 2013; 120:120–129.

6. Penjweini R, Loew H-G, Breit P, Kratky KW. Optimizing the antitumor selectivity of PVP-Hypericin re A549 cancer cells and HLF normal cells through pulsed blue light. Photodiagnosis Photodyn. Ther. 2013; 10(4):591–599. [PubMed: 24284116]
7. Penjweini R, Liu B, Kim MM, Zhu TC. Explicit dosimetry for 2-(1-hexyloxyethyl)-2-devinyl pyropheophorbide-a-mediated photodynamic therapy: macroscopic singlet oxygen modeling. Journal of biomedical optics. 2015; 20(12):128003. [PubMed: 26720883]
8. Zhu TC, Kim MM, Jacques SL, et al. Real-time treatment light dose guidance of Pleural PDT: an update. Proc. SPIE. 2015; 930809:930809–930806.
9. Zhu TC, Liang X, Kim MM, et al. An IR Navigation System for Pleural PDT. Frontiers in physics. 2015; 3(9):1–12.
10. Zhong H, Kim J, Li H, Nurushev T, Movsas B, Chetty IJ. A finite element method to correct deformable image registration errors in low-contrast regions. Physics in medicine and biology. 2012; 57(11):3499–3515. [PubMed: 22581269]
11. Liu B, Li J, Zhu TC. Deformable image registration for pleural photodynamic therapy. Proc. COMSOL. 2013
12. Shirzadi Z, Sadeghi-Naini A, Samani A. Toward in vivo lung's tissue incompressibility characterization for tumor motion modeling in radiation therapy. Medical physics. 2013; 40(5): 051902. [PubMed: 23635272]
13. Lai-Fook SJ, Hyatt RE. Effects of age on elastic moduli of human lungs. Journal of applied physiology. 2000; 89(1):163–168. [PubMed: 10904048]
14. Liu F, Tschumperlin DJ. Micro-mechanical characterization of lung tissue using atomic force microscopy. Journal of visualized experiments: JoVE. 2011; (54)

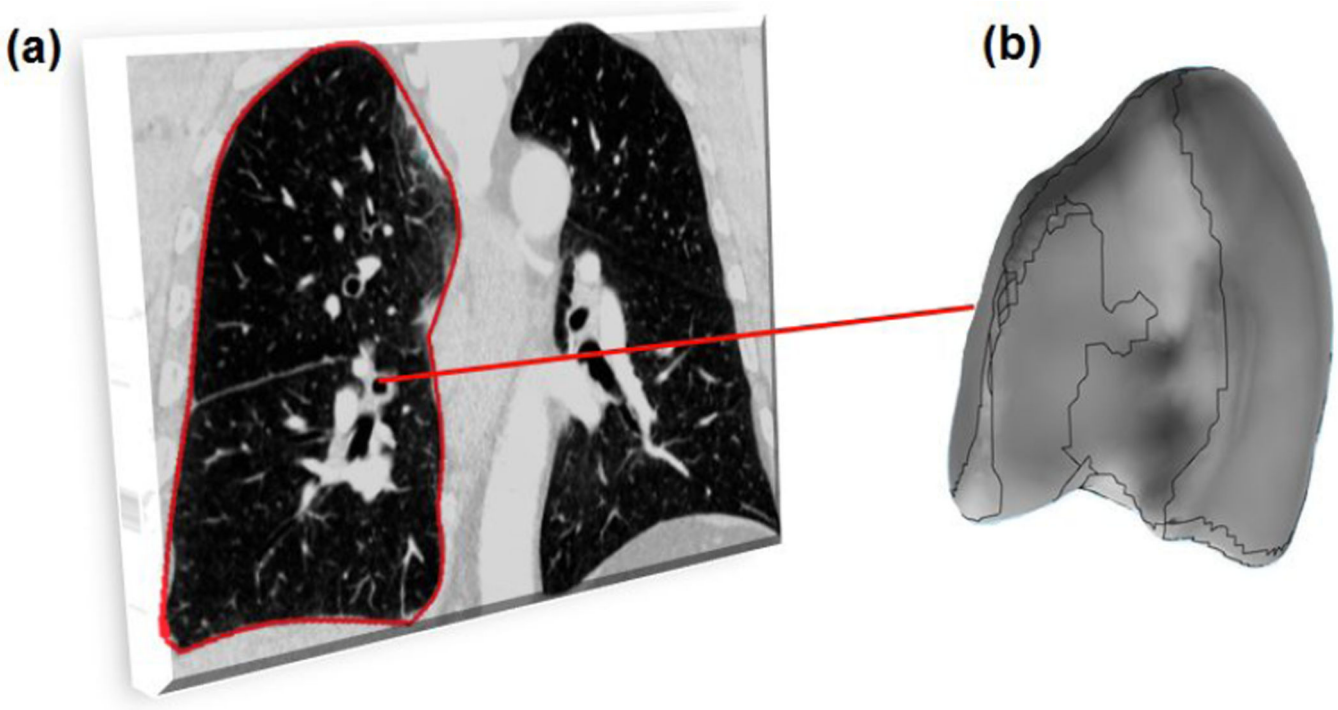

Figure 1.
(a) A series of computed tomography (CT) scans of the lungs before the surgery. (b) The three dimensional volume of the lung obtained from the CTs.

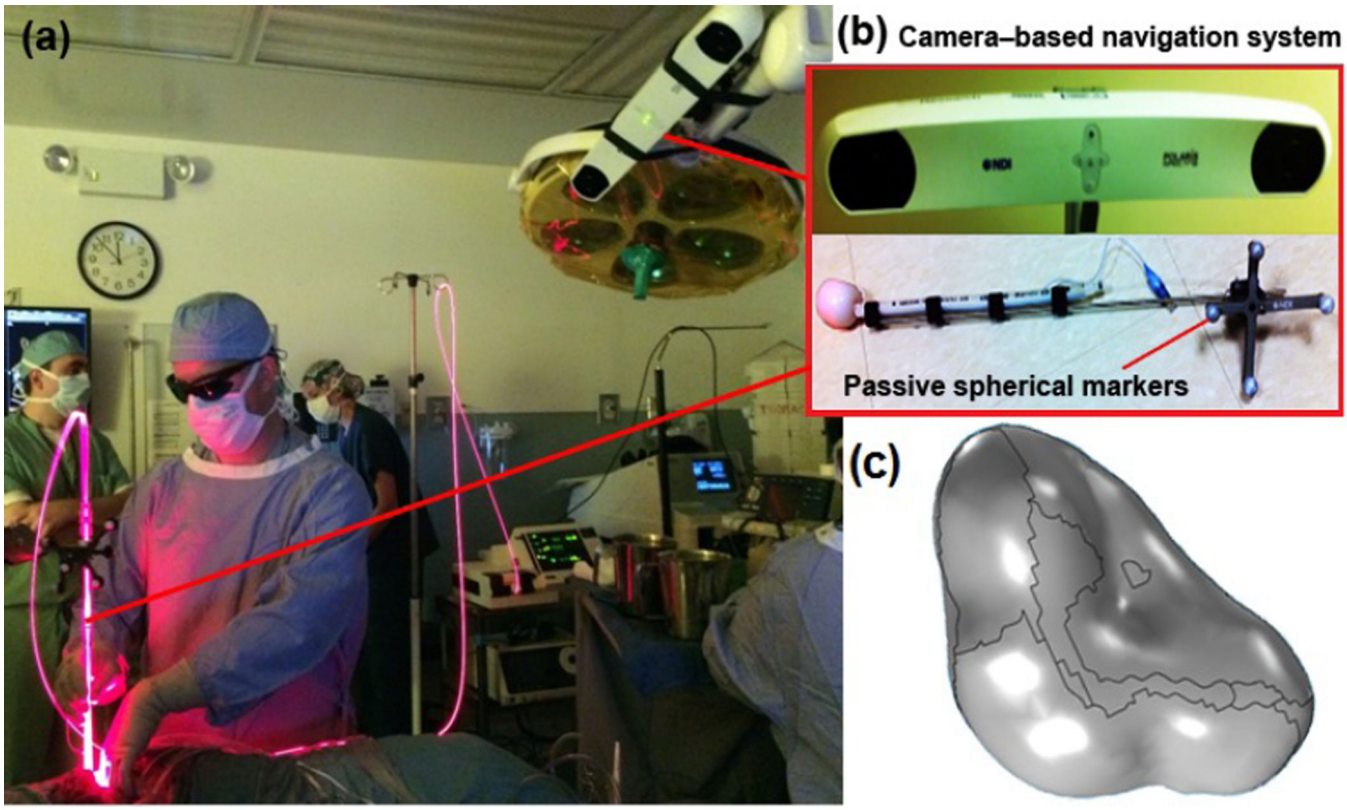

Figure 2.

(a) Infrared camera-based navigation system (NDI system) to monitor movement of a point in a 3D volume in the operating room. (b) A treatment wand with passive reflective spherical balls. (c) The volume of plural cavity obtained with the NDI system.

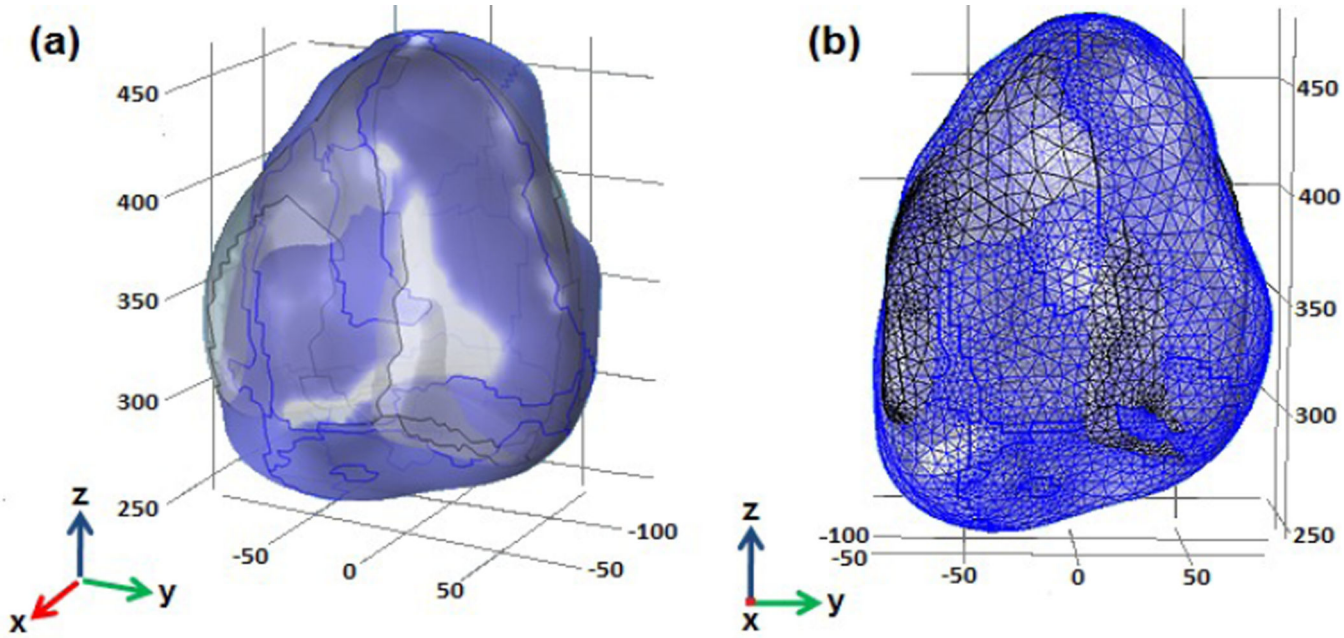

Figure 3.

(a) Registered and overlapped three dimensional contours in COMSOL. (b) The images presented with the grids for the finite element (FEM) analyses mesh. The gray volume presents the lung volume obtained from the CTs and the blue volume is the one obtained with the NDI system.

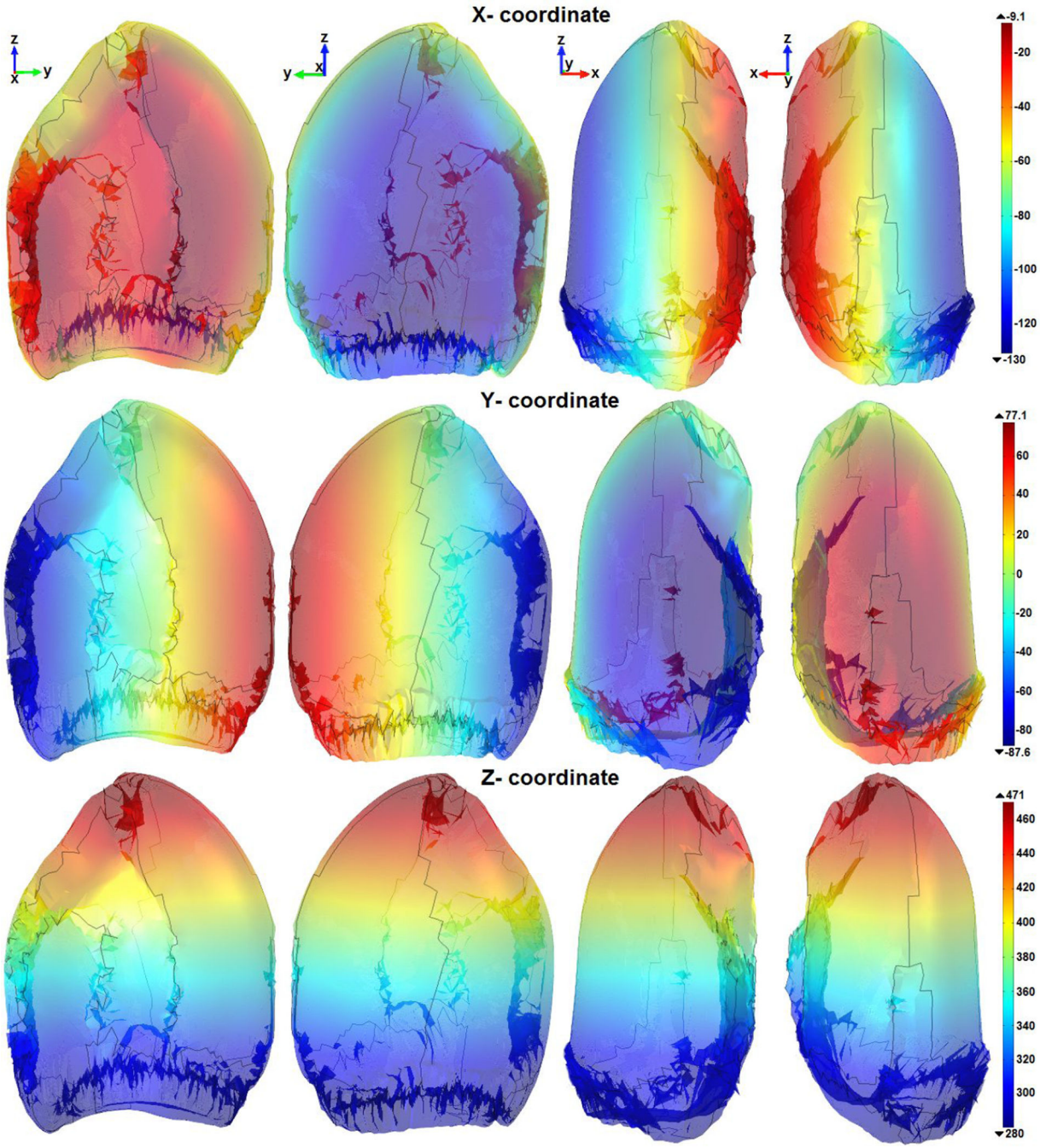

Figure 4.

Distortion of the CT volume in the X, Y and Z direction. Different colors represent different distortion magnitudes.

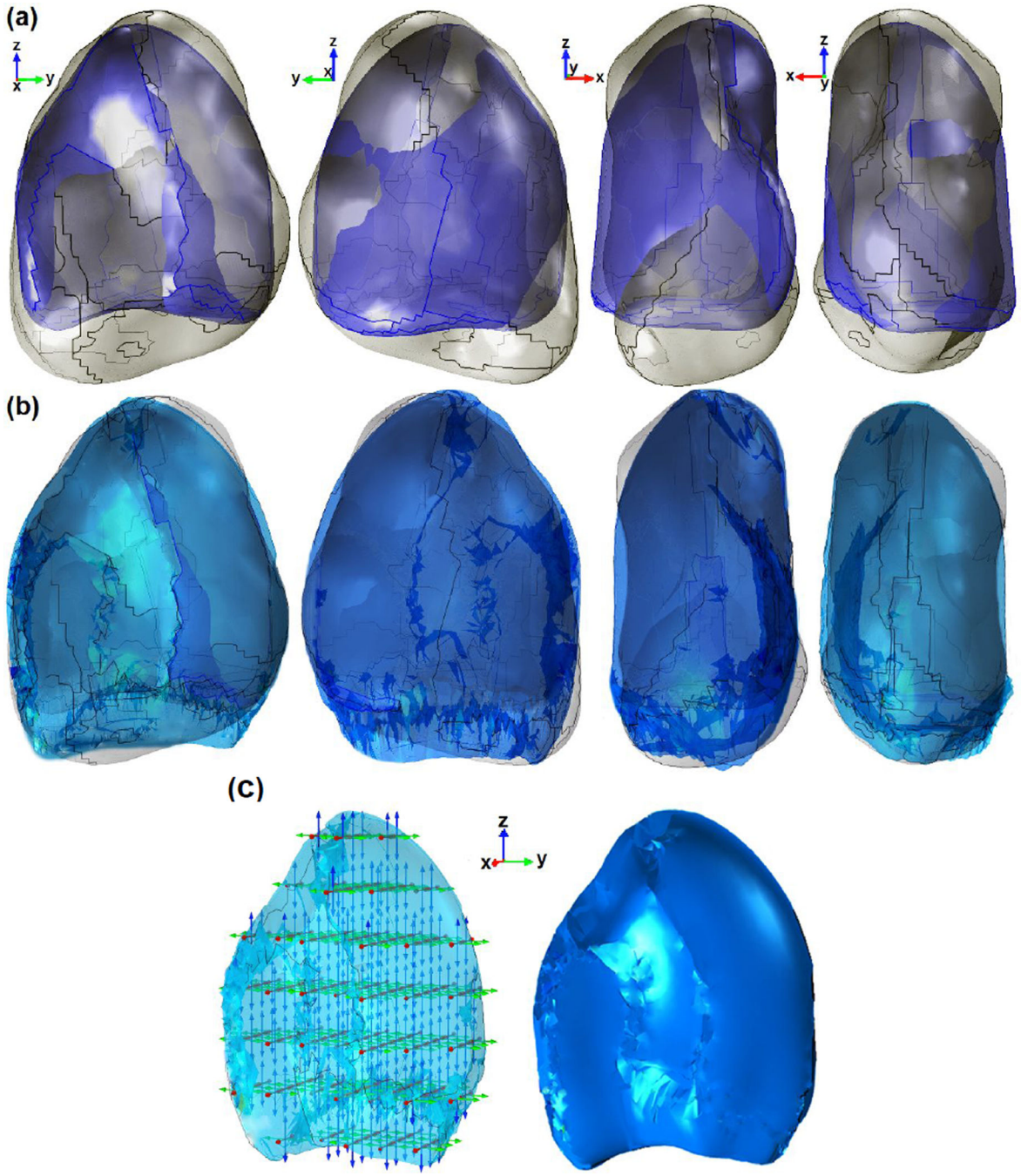

Figure 5.
(a) Original geometries of CT (blue) and NDI (gray) volumes before the deformation. (b) Deformed CT volume as compared to the fixed NDI volume. (c) Deformed CT volume and the stress vectors in X, Y and Z directions.

Table 1

Lung stress-strain material properties[12–14]

Poisson's value	Young's modulus (Pa)	Density (kg/m^3)	Mass (g)
0.36 ± 0.10	$(3 \pm 2) \times 10^3$	242 ± 10	353.5 ± 29.7

Table 2

Element statistics of the mesh generated for the CT domain.

Number of Tetrahedral elements	Number of Triangular elements	Edge elements	Vertex element	Minimum element quality	Average element quality	Element volume ratio	Mesh volume (cm^3)	Maximum growth rate	Average growth rate
132705	12728	979	147	0.13	0.74	2.74×10^{-5}	2072	3.40	1.70